

# Analysis of the ultimate noise performance of a mesoscopic cavity magnetic sensor

Massimo Macucci, Paolo Marconcini

*Dipartimento di Ingegneria dell'Informazione - Università di Pisa*

via Girolamo Caruso 16, 56122 Pisa, Italy

email address: macucci@mercurio.iet.unipi.it

***Index Terms***—1/f noise, magnetic sensors, III-V semiconductor materials

## I. ABSTRACT

Transport through a mesoscopic cavity divided into two identical dots by a tunnel barrier is characterized by constructive interference among symmetric paths, which has the effect to enhance the transmission through the cavity itself. Since this symmetry can be broken by a magnetic field, this device can be used as a magnetic field sensor. We first discuss a tradeoff for the definition of the most convenient geometrical dimensions and then, with the inclusion of the variance due to electrical noise (specifically flicker noise) we find the maximum sensitivity that can be achieved with this device.

## II. INTRODUCTION

A particular conductance enhancement effect that we discovered a few years ago [1] can in principle be applied to the implementation of magnetic field sensors. The effect is somewhat counterintuitive and consists in the strong enhancement of conductance through a barrier inserted in a 2-dimensional electron waveguide when two symmetric constrictions are added around the barrier [2] (see Fig. 1). While

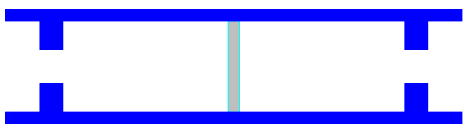


Fig. 1. Mesoscopic cavity with a barrier.

a first guess would be that the addition of the constrictions lowers the conductance, it can indeed increase it by more than an order of magnitude, as long as such constrictions are located exactly at the same distance on the two sides of the barrier. This conductance enhancement effect is the result of the constructive interference of symmetric paths. Thus it is sensitive to phase coherence, thereby setting a limit to the maximum size of the cavity for which the enhancement can be observed. Considering that many paths undergo a number of reflections within the cavity, the mean free path must be much longer than the cavity. Considering a mean free path of about  $160 \mu\text{m}$  (corresponding to the highest mobility achieved for a 2-dimensional electron gas of  $2 \times 10^7 \text{ cm}^2/(\text{V s})$ ) the

maximum cavity length for which a significant conductance enhancement effect is still visible is of the order of  $10 \mu\text{m}$  (allowing about 8 complete roundtrips in the cavity). Magnetic field breaks the symmetry of the paths [2] and therefore quenches the conductance enhancement effect: thus detection of a magnetic field is possible by looking at the conductance through a geometrically symmetric device. The conductance will have a maximum for zero magnetic field and will decrease as the magnetic field is increased. The achievable sensitivity is limited by the signal-to-noise ratio: here we perform an evaluation of the different noise contributions (thermal noise, shot noise, flicker noise) and determine the minimum value of the magnetic field that can be measured with a given accuracy.

The physical implementation of the device that we consider is based on a 2-dimensional electron gas in a GaAs/AlGaAs heterostructure, because of its high mobility: as already mentioned, it is essential to achieve the largest possible mobility since this allows the conductance enhancement effect to survive in the relatively large cavities that are needed to maximize the sensitivity. Indeed, as we will show in the following, the response of the device is substantially proportional to the magnetic flux threading the cavity, which implies that a tradeoff must be reached between two opposing requirements: the cavity should be large to thread more magnetic flux while it should be small to preserve phase coherence.

The cavity walls, as well as the barrier, can be defined with metal gates, which deplete the 2-dimensional electron gas outside the cavity and create the potential barrier. Such an implementation of the cavity has an important advantage with respect, for example, to a cavity obtained by means of etching: unavoidable geometrical asymmetries can, to a good extent, be compensated for by properly tuning the gate bias voltages [3]. Furthermore, also the height of the barrier can be controlled by tuning the voltage applied to the corresponding gate.

For all of the simulations that we will be presenting, we will assume a Fermi level of  $10 \text{ meV}$ , which is typical for the 2-dimensional electron gas in a GaAs/AlGaAs heterostructure.

## III. CAVITY GEOMETRY AND NUMERICAL TECHNIQUE

As shown in Fig. 1, the cavities that we will be considering are rectangular in shape, defined by means of two constrictions. The choice of a rectangular shape and of hard walls

leads to a significant reduction of the computational burden, while not appreciably affecting the results.

Also the constrictions are abrupt and with hard walls, and their extension in the longitudinal direction is not relevant, as long as it is large enough to make coupling via evanescent modes negligible.

The barrier is assumed to be uniform in the transverse direction and to have a rectangular cross-section in the longitudinal direction.

We compute the conductance through the cavity as a function of the magnetic field, keeping the Fermi level constant at the previously mentioned value of 10 meV. Calculations are performed at zero temperature within the Landauer-Büttiker approach to transport in mesoscopic systems. The evaluation of conductance is thus turned into the solution of a scattering problem across the structure. Considering that a bias of a few millivolts between the input and output leads of the cavity will be needed to reliably measure the device conductance, the transmission calculation is performed by averaging a few tens of energy values over an interval of a few millielectronvolts. This smooths out the transmission curves, which would otherwise present some rapid oscillations, as a result of the very large number of modes propagating in the cavity (of the order of 180).

The transmission is computed with a recursive Green's function approach [4]–[6], operating in real space in the longitudinal direction and in the mode space in the transverse direction. The cavity is subdivided into a series of slices, within each of which the potential can be assumed to be constant. In the absence of magnetic field, just 5 sections plus the input and output leads would be sufficient (2 for the constrictions, 2 for the halves of the cavity and 1 for the barrier), but when magnetic field is present we need a much larger number of slices. This is because we choose a gauge in which the only non-vanishing component of the vector potential is along the transverse direction [7]: on the one hand this makes the calculation of the transverse eigenfunctions much easier than with different choices of gauge (in this case the transverse eigenfunctions are obtained multiplying the ones for no magnetic field by a proper phase factor); on the other hand this approach requires that each slice is threaded by a flux less than a flux quantum, and therefore we had to use up to a few hundred slices. The magnetic field is assumed to be applied to the constrictions, the cavity, and part of the leads, while it is set to zero at the lead locations between which transmission matrices are computed, in order to make their computation easier. Between such lead locations and the constrictions the magnetic field is ramped linearly.

#### IV. CHOICE OF CAVITY PARAMETERS

As discussed in the introduction, the choice of the cavity size is a result of a trade-off between the requirement of threading the largest possible magnetic flux and that of preserving phase coherence even for paths that undergo a relatively large number of reflections. In Fig. 2 we report the conductance through cavities 4  $\mu\text{m}$  wide and with a length

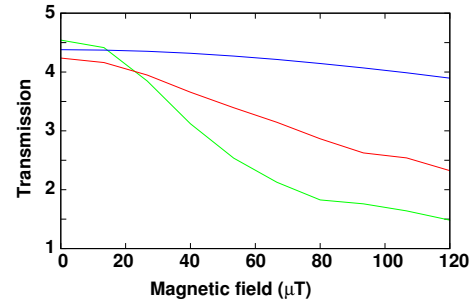


Fig. 2. Transmission vs. magnetic field for different cavity lengths.

of 4  $\mu\text{m}$  (blue curve), 8  $\mu\text{m}$  (red curve), and 16  $\mu\text{m}$  (green curve) as a function of magnetic field. The constrictions are assumed to be symmetric, 340 nm wide and 400 nm long, while the barrier is 12 nm thick and with a height of 45 meV. It is apparent that increasing the length of the cavity

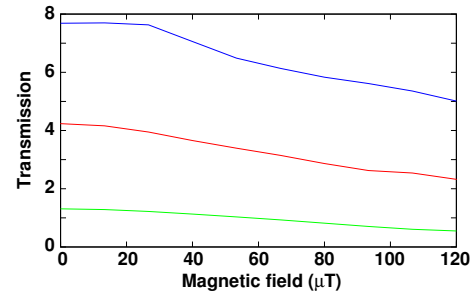


Fig. 3. Transmission vs. magnetic field for different barrier widths.

the slope of the transmission vs. magnetic field increases, but it is not recommendable to go beyond 8  $\mu\text{m}$ , even at very low temperatures, in order to prevent excessive decoherence. We then try varying the width of the barrier, keeping, for the rest, the same parameters as in the previous calculation. In Fig. 3(a) we report the computed transmission vs. magnetic field for a 4  $\mu\text{m} \times 8 \mu\text{m}$  cavity for different barrier thicknesses: 8 nm (blue curve), 12 nm (red curve) and 16 nm (green curve). It is apparent that a thicker barrier leads to a reduced slope, but, at the same time, the conductance enhancement ratio for the 8 nm barrier is decreased, therefore for our evaluations we choose a 12 nm thick barrier.

We have further explored the parameter space looking at the behavior of the conductance as a function of magnetic field for different values of the constriction width. Results are reported in Fig. 4: we notice that the largest conductance enhancement is observed for a width of 340 nm, while for smaller (200 nm) or larger (1000 nm) widths the conductance drops. Further increasing or decreasing the width of the constrictions a strong reduction of the conductance is observed. On the basis of the results shown so far, we have decided to take into consideration, for our analysis, a cavity that is 4  $\mu\text{m}$  wide, 8  $\mu\text{m}$  long, with 340 nm constrictions, a 12 nm thick and 45 meV high barrier.

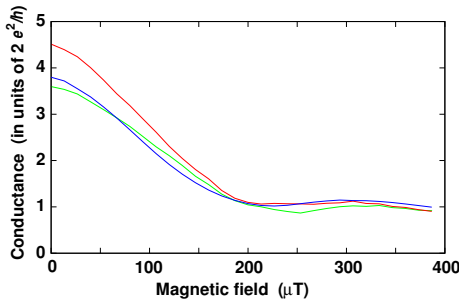


Fig. 4. Transmission as a function of magnetic field for different constriction widths: the red curve is for a constriction width of 340 nm, the blue curve for a width of 1000 nm and the green curve for a width of 200 nm.

## V. SIGNAL TO NOISE RATIO AND SENSITIVITY

We take into consideration thermal, shot, and flicker noise. Thermal noise has a power spectral density  $S_{th} = 4kTR_{dev}$  (which depends only on temperature and on the value of the device resistance  $R_{dev}$ ). Since the output signal consists of the current flowing for a given applied bias voltage, it can be increased proportionally to the bias voltage, while thermal noise is not affected by the bias voltage, unless a value causing non-negligible self-heating is reached. Thus thermal noise does not represent an actual limiting factor for sensitivity.

Let us then consider the contribution of shot noise: the noise power spectral density  $S_{sh} = 2qI$  increases linearly with the bias current, while the signal power increases quadratically. Thus the signal-to-noise ratio associated with shot noise increases as the bias voltage is increased.

Finally, we consider the contribution from flicker noise: the flicker noise power spectral density increases quadratically with the bias current (according the Hooge relationship:  $S_{fl} = \alpha_H I^2 / (Nf)$ , where  $\alpha_H$  is the Hooge constant,  $I$  the bias current and  $N$  the number of charge carriers). As a result, the flicker noise power spectral density has the same, quadratic, dependence on the applied voltage, and therefore the signal-to-noise ratio cannot be improved by increasing the bias voltage. Thus flicker noise represents the fundamental limitation to the achievable sensitivity. In particular, it has to be pointed out that, contrary to what can be sometimes found in the literature, using an AC bias does not help, because in such a case the  $1/f$  spectrum will just be translated around the bias frequency. At zero frequency (or around the frequency of the AC bias) the spectrum diverges, but this does not involve that the noise power will become infinite, because the observation time is finite. A finite observation time implies that the contribution from the the lower frequency components is limited, and therefore a finite variance on the measured value is achieved. The standard deviation (i.e. the square root of such a variance) can be evaluated with the approach due to Allan [8], [9], which, in the case of flicker noise with a power spectral density  $S_{I_{fl}} = \theta/f$  is given by

$$\sigma = \sqrt{1.386 \times \theta} \quad (1)$$

We notice that the slope of the transmission curve vanishes when approaching the origin, which leads to a loss of sensitivity for very small values of the magnetic field. This can be circumvented by applying a small constant magnetic field bias of about 100  $\mu\text{T}$ , in such a way as to operate in the region with the largest derivative.

Unfortunately, it has not been possible to find in the literature a direct measurement of the flicker noise power spectral density for a device such as the one we have presented or just for a mesoscopic cavity. However, we can perform some estimate of the low-frequency noise in this structure. First of all, we expect, based on Hooge's relationship, that the most relevant contribution to flicker noise will come from the regions with the smallest number of carriers, therefore from the constrictions. To obtain an estimate of the constriction noise we can either compute the number of carriers therein and use Hooge's formula, with a value for  $\alpha_H$  taken from the literature for a 2-dimensional electron gas in a GaAs/AlGaAs heterostructure, or collect from the literature the flicker noise data measured on quantum point contacts obtained for GaAs/AlGaAs heterostructures. In a previous study [10] we used the former approach, but we believe the latter to be more reliable, because a value of the Hooge coefficient obtained in rather different experimental conditions cannot be applied with confidence to our problem. From Ref. [11] we find that  $S_{I_{fl}}/I^2 = 10^{-10} \text{ Hz}^{-1}$  at 100 Hz. Thus, for a current of, for example, 0.3  $\mu\text{A}$  the spectrum of the flicker noise power spectral density should be  $S_{I_{fl}} = 9 \cdot 10^{-22} \text{ A}^2/f$ .

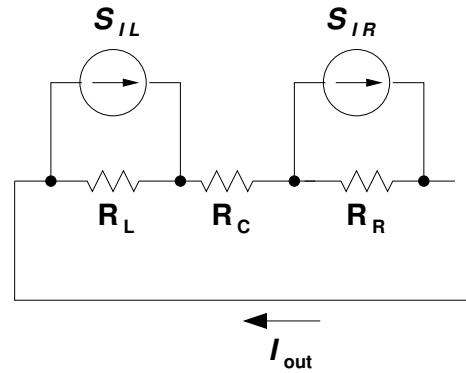


Fig. 5. Simplified circuit representation for the cavity, with the two noise sources corresponding to the constrictions.

In order to compute the resulting overall noise, we can represent the device as the series of two noisy resistors, representing the two constrictions, separated by a resistor representing the mesoscopic cavity (see Fig. 5). Notice that since the cavity contains a much greater number of carriers than the constrictions, according to Hooge's formula we can neglect its noise contribution and represent it with a noiseless resistance. If the left and right contacts of the sensor are connected through an external conductor, the noise in this conductor will result from the superposition of the effects of the flicker noise generators (assumed to be uncorrelated)

corresponding to the two constrictions (with power spectral density  $S_{I_L}$  and  $S_{I_R}$ , respectively). Therefore, the noise power spectral density in the outer conductor  $S_{I_{out}}$  will be equal to

$$S_{I_{out}} = S_{I_L} \frac{R_L^2}{(R_L + R_C + R_R)^2} + S_{I_R} \frac{R_R^2}{(R_L + R_C + R_R)^2}. \quad (2)$$

If the constrictions are identical, we can consider  $R_L = R_R = R$  and  $S_{I_L} = S_{I_R} = S_{I_{fl}}$ . A worst case estimate can be obtained neglecting  $R_C$ : in this case, we have that  $S_{I_{out}} = S_{I_{fl}}/2$ , which in our case (with a current of  $0.3 \mu\text{A}$ ) means  $S_{I_{out}} = \theta/f = 4.5 \cdot 10^{-22} \text{ A}^2/\text{f}$ . Using Allan's approach, this corresponds to a standard deviation  $\sigma = \sqrt{1.386} \theta = 25 \text{ pA}$ .

As we have previously anticipated, it is preferable to operate the device with a small constant magnetic field bias of about  $100 \mu\text{T}$ , in order to be in the condition for which the transmission curve as a function of magnetic field has the largest derivative ( $\Delta G/\Delta B \approx -1.25 \Omega^{-1}/\text{T}$ , from Fig. 4). For this value of the magnetic field we have a conductance  $G_0 = 0.15 \text{ m}\Omega^{-1}$ , which means that, in order to obtain the considered bias current  $I_0 = 0.3 \mu\text{A}$ , a bias voltage  $V_0 = I_0/G_0 = 2 \text{ mV}$  has to be applied to the sensor.

With the addition of noise, the measured current values will be scattered, but will mainly fall within an interval of  $\pm 3\sigma$ , i.e. in our case  $75 \text{ pA}$ , around the expected value. Therefore, an accuracy of 10% in the measurement will be obtained only for  $\Delta I > 10 \cdot 75 \text{ pA} = 0.75 \text{ nA}$ . The current variation  $\Delta I$  is related to the conductance variation  $\Delta G$  and thus to the magnetic field variation  $\Delta B$  that has generated it by the following relation:

$$\Delta I = V_0 \Delta G = V_0 \frac{\Delta G}{\Delta B} \Delta B. \quad (3)$$

Substituting the values of  $\Delta I$ ,  $V_0$  and  $\Delta G/\Delta B$ , we obtain a value  $\Delta B \approx 300 \text{ nT}$ , which therefore represents an estimate of the sensitivity of the sensor.

## VI. CONCLUSION

We have estimated the maximum sensitivity achievable with a magnetic field sensor consisting of a mesoscopic cavity with a potential barrier in the middle. The constructive interference among paths, which, in the presence of phase coherence, dominates transmission in this geometrically symmetric device are progressively washed out by the presence of an orthogonal magnetic field. We have first focused on the choice of a geometry suitable for the best detection sensitivity, by reaching a tradeoff between the requirement of collecting the largest possible magnetic flux and the requirement of preserving phase coherence for the paths that perform up to about 15 bounces within the cavity. We have then made an estimate of the power spectral density of flicker noise in the considered device, after reaching the conclusion that it represents the main limitation to the achievable sensitivity. Using an approach based on Allan's variance we have finally evaluated a maximum possible sensitivity of the order of  $300 \text{ nT}$ .

## ACKNOWLEDGMENT

This work was partially supported by the Italian Ministry of Education and Research (MIUR) in the framework of the CrossLab project (Departments of Excellence).

## REFERENCES

- [1] M. Macucci and P. Marconcini, "Tunneling enhancement through a barrier surrounded by a mesoscopic cavity," *Journal of Computational Electronics*, vol. 6, p. 203, 2007, DOI: 10.1007/s10825-006-0111-9.
- [2] R. S. Whitney, P. Marconcini, and M. Macucci, "Huge conductance peak caused by symmetry in double quantum dots," *Phys. Rev. Lett.*, vol. 102, p. 186802, 2009, DOI: 10.1103/PhysRevLett.102.186802.
- [3] M. Totaro, P. Marconcini, D. Logoteta, M. Macucci, and R. S. Whitney, "Effect of imperfections on the tunneling enhancement phenomenon in symmetric double quantum dots," *J. Appl. Phys.*, vol. 107, p. 043708, 2010, DOI: 10.1063/1.3309747.
- [4] D. J. Thouless and S. Kirkpatrick, "Conductivity of the disordered linear chain," *J. Phys. C*, vol. 14, p. 235, 1981, DOI: 10.1088/0022-3719/14/3/007.
- [5] F. Sols, M. Macucci, U. Ravaioli, and K. Hess, "Theory for a quantum modulated transistor," *J. Appl. Phys.*, vol. 66, p. 3892, 1989, DOI: 10.1063/1.344032.
- [6] M. Macucci, A. Galick, and U. Ravaioli, "Quasi-three-dimensional Greens-function simulation of coupled electron waveguides," *Phys. Rev. B*, vol. 52, p. 5210, 1995, DOI: 10.1103/PhysRevB.52.5210.
- [7] M. Macucci, P. Marconcini, "Shot noise suppression due to a magnetic field in disordered conductors," *J. Comput. Electron.*, vol. 14, p. 107, 2015, DOI: 10.1007/s10825-014-0647-z.
- [8] D. W. Allan, "Statistics of atomic frequency standards," *Proc. IEEE*, vol. 54, p. 221, 1966, DOI: 10.1109/PROC.1966.4634.
- [9] G. Giusi, G. Scandurra, C. Ciofi, and C. Pace, "Long term stability estimation of DC electrical source from low frequency noise measurements," in *Proceedings of SPIE*, vol. 5470, *Noise in Devices and Circuits II*, 2004, p. 470, DOI: 10.1117/12.547137.
- [10] M. Macucci and P. Marconcini, "Study of the Signal to Noise Ratio of a Double-Dot Magnetic Detector," in *2018 IEEE 13th Nanotechnology Materials and Device Conference, NMDC 2018*, Portland, OR, 2018, article n. 8605875, DOI: 10.1109/NMDC.2018.8605875.
- [11] Y. P. Li, D. C. Tsui, J. J. Heremans, J. A. Simmons, and G. W. Weimann, "Low-frequency noise in transport through quantum point contacts," *Appl. Phys. Lett.*, vol. 57, p. 774, 1990, DOI: 10.1063/1.104094.